Special Relativity and Reactions with Unstable Nuclei

C.A. Bertulani

Department of Physics, University of Arizona, Tucson, Arizona 85721

Abstract. Dynamical relativistic effects are often neglected in the description of reactions with unstable nuclear beams at intermediate energies ($E_{Lab} \approx 100$ MeV/nucleon). Evidently, this introduces sizable errors in experimental analysis and theoretical descriptions of these reactions. This is particularly important for the experiments held in GANIL/France, MSU/USA, RIKEN/Japan and GSI/Germany. I review a few examples where relativistic effects have been studied in nucleus-nucleus scattering at intermediate energies.

1. INTRODUCTION

The number of radioactive beam facilities are growing fast around the world. Some of these facilities use the fragmentation technique, with secondary beams in the energy range $E_{Lab} \approx 100$ MeV/nucleon. Examples are the facilities in GANIL/France, MSU/USA, RIKEN/Japan and GSI/Germany. Relativity, an obviously important physics concept [1], is often neglected in calculations aiming at relating the reaction mechanisms to the internal structure of the projectiles. For example, popular DWBA codes (FRESCO, ECIS, DWUCK, etc.) useful in the analysis of nuclear reactions, include relativity only in kinematic relations. The effects of relativity in the reaction dynamics (i.e. the interaction) is not accounted for because these codes were intended for lower energies. It is also important to notice that the inclusion of relativistic effects in the nucleus-nucleus dynamics is a very difficult task. A fully covariant treatment of the nuclear many-body scattering (with inclusion of retardation effects between all nucleons) is not possible without approximations.

In this short article I will review a few examples where relativistic effects have been included in nuclear reactions at intermediate energies. It is worthwhile to observe that after 100 years of relativity [1] this still remains a challenge in many aspects.

2. SEMICLASSICAL METHODS AND ELASTIC SCATTERING

Semiclassical methods are a very popular tool for the description of nucleus-nucleus collisions at high energies. As an example, I cite the Coulomb excitation mechanism, in which the inelastic cross section can be factorized as

$$\frac{d\sigma_{i \to f}}{d\Omega} = \left(\frac{d\sigma}{d\Omega}\right)_{\text{el}} P_{i \to f}, \tag{1}$$

where $P_{i \to f}$ is the probability for a nuclear transition between the states i and f when the nuclei scatter through an angle Ω. The collision dynamics enters here in two distinct ways: in the calculation of $P_{i \to f}$ and $(d\sigma/d\Omega)_{\text{el}}$. Let us forget about $P_{i \to f}$ for a moment and let us investigate $(d\sigma/d\Omega)_{\text{el}}$. The question here is what is the error done by measuring the number of particles scattered to Ω and using the Rutherford formula for $(d\sigma/d\Omega)_{\text{el}}$. This has been investigated in ref. [2].

A system of two point charges interacting electromagnetically and moving at low velocities can be described by an approximate Lagrangian which depends only on the degrees of freedom of the particles neglecting those related to the electromagnetic field (the Darwin Lagrangian's). In this approximation it is possible to separate the degrees of freedom associated with the relative position r and relative velocity v of the particles from the center of mass degrees of freedom. For a system of particles with different masses this approximation is only possible up to the c^{-2} order, whereas for a system with equal charge-to-mass ratio (with $Z_1 e/m_1 = Z_2 e/m_2$) the approximation goes up to order c^{-4}. Using Lagrange's equation of motion, it is then straightforward to obtain a numerical result for the deflection
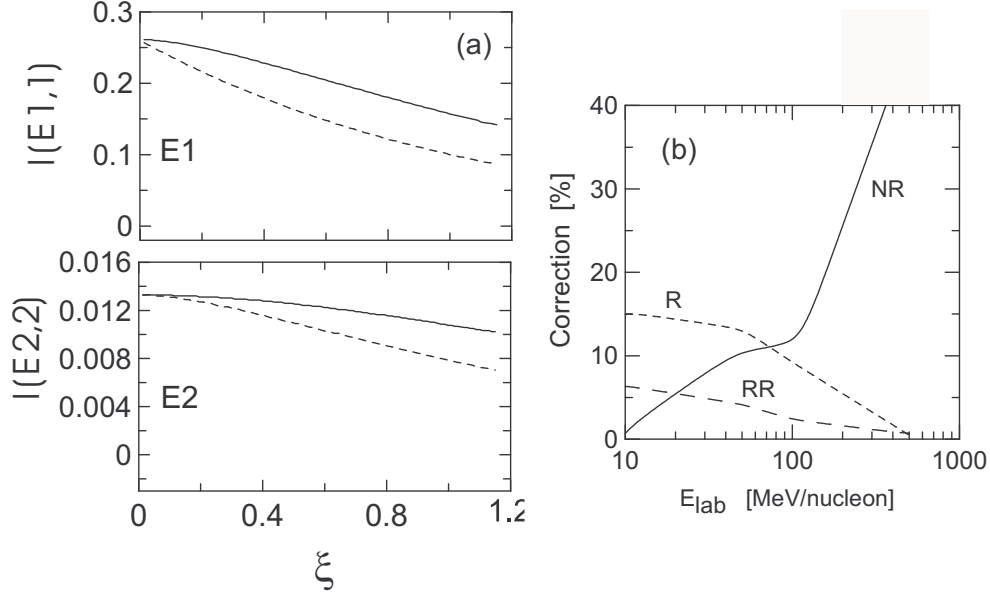
FIGURE 1. (a) Upper panel: Real part (solid line) of the orbital integral $I(E1,1)$ for $\gamma = 1.1$ ($E_{lab} \simeq 100$ MeV/nucleon), calculated with a theory containing both retardation and relativistic corrections to the Coulomb trajectory. The approximation used in ref. [5], neglecting relativistic corrections to the Coulomb trajectory, is shown by the dashed line. Lower panel: Same plot, but for the orbital integral $I(E2,2)$. (b) Percentage correction in the calculation of the cross sections for Coulomb excitation of the 0.89 MeV state in ^{40}S + ^{197}Au collisions as a function of the bombarding energy. The solid line (NR) corresponds to the use of the non-relativistic orbital integrals [4] compared to the "exact" calculation of ref. [9]. The same is plotted for the other two cases: (R) with retardation effects only [5], and (RR) with the retardation effects plus an approximate recoil correction [5]. For more details, see ref. [5].

angle and the elastic cross section. Explicit expressions for these Lagrangians are given in ref. [2]. The authors show that the scattering angle increases by up to 6% when relativistic corrections are included in ^{208}Pb $+^{208}$Pb collisions at 100 MeV/nucleon. The effect on the elastic scattering cross section is even more drastic: $\approx 13\%$ for center-of-mass scattering angles around 0-4 degrees.

Another result obtained in ref. [2] is that the effects of relativity can be taken into account in a much simpler way when the projectile is a light particle scattering on a heavy target (e.g., ^{11}Li $+^{208}$Pb). In this case, the main contribution of relativistic corrections (up to 80% of the total effect) is due to the changes in masses, an easily implementable correction. Only about 20% of the relativistic effects are due to magnetic interactions and retardation. Then, a good approximation for the elastic scattering is given by

$$\left(\frac{d\sigma}{d\Omega}\right)_{el}(\beta,\Theta) = \left[\frac{Z_1 Z_2 e^2}{2mc^2\beta^2 \sin^2(\Theta/2)}\right]^2 \left[1 - h(\Theta)\beta^2 + \mathscr{O}(\beta^2)\right] \tag{2}$$

where

$$h(\Theta) = 1 + \frac{1}{2}[1 + (\pi - \Theta)\cot\Theta]\tan^2\frac{\Theta}{2}, \qquad \Theta = \pi - 2\frac{\eta}{\sqrt{\eta^2 - \beta^2}}\arctan\sqrt{\eta^2 - \beta^2},$$

with $\eta = \beta Lc/Z_1 Z_2 e^2$, L being the angular momentum of the system, and $\beta = v/c$. The function $h(\Theta)$ is always positive for the relevant scattering angles. Therefore one concludes that the relativistic corrections in the elastic Coulomb cross section are always negative if they are parametrized as a function of the initial velocity. On the other hand if one fixes the initial kinetic energy, instead of the velocity, the corrections will be always positive, as shown in ref. [2].

The study mentioned above is useful for an analysis of experimental data on inelastic nucleus-nucleus scattering in intermediate energy collisions. The extension of these calculations to all orders in β is an intriguing problem and an appropriate tool could be the use of the action-at-a-distance electrodynamics of Fokker, Wheeler and Feynman [3]. Certainly, more studies in this direction are needed and the present focus on nuclear reactions at intermediate energies seem to be a good opportunity to investigate such effects.

3. ANOTHER TRACTABLE CASE: COULOMB EXCITATION

The theory of Coulomb excitation in low-energy collisions is very well understood [4]. It has been used and improved for over thirty years to infer electromagnetic properties of nuclei and has also been tested in experiments to a high level of precision. A large number of small corrections are now well known in the theory and are necessary in order to analyze experiments on multiple excitation and reorientation effects.

In the case of relativistic heavy ion collisions pure Coulomb excitation may be distinguished from the nuclear reactions by demanding extreme forward scattering or avoiding the collisions in which violent reactions take place. The Coulomb excitation of relativistic heavy ions is thus characterized by straight-line trajectories with impact parameter b larger than the sum of the radii of the two colliding nuclei. A detailed calculation of relativistic electromagnetic excitation on this basis was performed by Winther and Alder [5]. As in the non-relativistic case, they showed how one can separate the contributions of the several electric ($E\lambda$) and magnetic ($M\lambda$) multipolarities to the excitation. Later, it was shown that a quantum theory for relativistic Coulomb excitation leads to minor modifications of the semiclassical results [6]. In Refs. [7, 8] the inclusion of relativistic effects in semiclassical and quantum formulations of Coulomb excitation was fully clarified.

Recently, the importance of relativistic effects in Coulomb excitation of a projectile by a target with charge Z_2, followed by gamma-decay in nuclear reactions at intermediate energies was studied in details. The Coulomb excitation cross section is given by

$$\frac{d\sigma_{i\to f}}{d\Omega} = \left(\frac{d\sigma}{d\Omega}\right)_{el} \frac{16\pi^2 Z_2^2 e^2}{\hbar^2} \sum_{\pi\lambda\mu} \frac{B(\pi\lambda, I_i \to I_f)}{(2\lambda+1)^3} \mid S(\pi\lambda,\mu) \mid^2, \qquad (3)$$

where $B(\pi\lambda, I_i \to I_f)$ is the reduced transition probability of the projectile nucleus, $\pi\lambda = E1, E2, M1,\ldots$ is the multipolarity of the excitation, and $\mu = -\lambda, -\lambda+1,\ldots,\lambda$. The orbital integrals $S(\pi\lambda,\mu)$ contain the information about relativistic corrections on the relative motion between the nuclei, as well as the relativistic effects on the excitation mechanism (e.g. retarded Coulomb interaction). Inclusion of absorption effects in $S(\pi\lambda,\mu)$ due to the imaginary part of an optical nucleus-nucleus potential where worked out in ref. [8]. These orbital integrals depend on the Lorentz factor $\gamma = (1 - v^2/c^2)^{-1/2}$, with c being the speed of light, on the multipolarity $\pi\lambda\mu$, and on the adiabacity parameter $\xi(b) = \omega_{fi} b/\gamma v < 1$, where $\omega_{fi} = (E_f - E_i)/\hbar$ is the excitation energy (in units of $\hbar$) and b is the impact parameter. It is often more convenient to write the orbital integrals in another form, e.g. $S(E\lambda,\mu) = \frac{\mathscr{C}_{\lambda\mu}}{va^\lambda} I(E\lambda,\mu)$, where $\mathscr{C}_{\lambda\mu}$ is a geometrical factor, depending only on λ and μ, $a = Z_1 Z_2 e^2/\gamma mv^2$, and $I(E\lambda,\mu)$ is now the orbital integral in an dimensionless form.

Figure 1(a) (from [9]) shows the effect of relativity on the Coulomb interaction and classical trajectory corrections in nuclear collisions at intermediate collisions. The comparison is made in terms of the variable ξ which is the appropriate variable for high energy collisions. Only for $\xi \ll 1$ the expressions in the relativistic limit reproduce the correct behavior of the orbital integrals.

TABLE 1. Coulomb excitation cross sections of the first excited state in ^{38,40,42}S and ^{44,46}Ar projectiles at 10, 50 100 and 500 MeV/nucleon incident on gold targets. The numbers inside parenthesis and brackets were obtained with pure non-relativistic and straight-line relativistic calculations, respectively. The numbers at the center are obtained with the "full" account of relativistic effects, as explained in ref. [9].

Nucleus	E_x [MeV]	B(E2) [e^2fm^4]	10 MeV/A σ_C [mb]	50 MeV/A σ_C [mb]	100 MeV/A σ_C [mb]	500 MeV/A σ_C [mb]
^{38}S	1.29	235	(492) 500 [651]	(80.9) 91.7 [117]	(40.5) 50.1 [57.1]	(9.8) 16.2 [16.3]
^{40}S	0.89	334	(877) 883 [1015]	(145.3) 162 [183]	(76.1) 85.5 [93.4]	(9.5) 20.9 [21.]
^{42}S	0.89	397	(903) 908 [1235]	(142.7) 158 [175]	(65.1) 80.1 [89.4]	(9.9) 23.2 [23.4]
^{44}Ar	1.14	345	(747) 752 [985]	(133) 141 [164]	(63.3) 71.7 [80.5]	(8.6) 17.5 [17.6]
^{46}Ar	1.55	196	(404) 408 [521]	(65.8) 74.4 [88.5]	(30.2) 37.4 [41.7]	(5.72) 10.8 [11]

Table 1 shows the effects of relativistic corrections in the collision of the radioactive nuclei ^{38,40,42}S and ^{44,46}Ar on gold targets. These reactions have been studied at $E_{lab} \sim 40$ MeV/nucleon at the MSU facility [10]. Table 1 shows the Coulomb excitation cross sections of the first excited state in each nucleus as a function of the bombarding energy per nucleon. The cross sections are given in milibarns. The numbers inside parenthesis and brackets were obtained with

pure non-relativistic [4] and relativistic calculations [5], respectively. The minimum impact parameter is chosen so that the distance of closest approach corresponds to the sum of the nuclear radii in a collision following a Rutherford trajectory. One observes that at 10 MeV/nucleon the relativistic corrections are important only at the level of 1%. At 500 MeV/nucleon, the correct treatment of the recoil corrections is relevant on the level of 1%. Thus the non-relativistic treatment of Coulomb excitation [4] can be safely used for energies below about 10 MeV/nucleon and the relativistic treatment with a straight-line trajectory [5] is adequate above about 500 MeV/nucleon. However at energies around 50 to 100 MeV/nucleon, accelerator energies common to most radioactive beam facilities (MSU, RIKEN, GSI, GANIL), it is very important to use a correct treatment of recoil and relativistic effects, both kinematically and dynamically. At these energies, the corrections can add up to 50%. These effects were also shown in Ref. [7] for the case of excitation of giant resonances in collisions at intermediate energies.

We conclude that a reliable extraction useful nuclear properties, like the electromagnetic response (B(E2)-values, γ-ray angular distribution, etc.) from Coulomb excitation experiments at intermediate energies requires a proper treatment of special relativity. The effect is highly non-linear, i.e. a 10% increase in the velocity might lead to a 50% increase (or decrease) of certain physical quantities.

4. STRONG INTERACTION: GLAUBER, DWBA AND SEMICLASSICAL METHODS

The treatment of the strong interaction in nucleus-nucleus collisions at intermediate and high energies is evidently much more complicated than the case of Coulomb excitation, described in the previous section. Fortunately, many direct nuclear processes, e.g. nucleon knockout, or stripping, elastic breakup (diffraction dissociation), etc, are possible to study using the optical limit of the Glauber theory, in which the nuclear ground-state densities and the nucleon-nucleon total cross sections are the main input. In fact, this method has become one of the main tools in the study of nuclei far from stability [11]. The reason is that the eikonal (or Glauber) methods only use the dependence of the scattering matrices, $S(b)$, on the transverse direction, b. Transverse directions are always Lorentz invariants. The reason for using $S(b)$, instead of $S(\mathbf{r})$, traces back to the eikonal scattering wavefunction at the asymptotic region $(r \longrightarrow \infty)$,

$$\Psi_{scatt} = S(b) \, \exp(i\mathbf{k} \cdot \mathbf{r}) \,, \tag{4}$$

where $\mathbf{k}$ is the particle's momentum, and $\mathbf{r}$ its position. Obviously, the plane wave part of eq. 4 is Lorentz invariant. The S-matrix in eq. 4 is $S = \exp\{i\chi(b)\}$, where $\chi(b)$ is the eikonal phase-shift, given in terms of the interaction potential V by

$$\chi = -\frac{1}{\hbar v} \int_{-\infty}^{\infty} dz \, V(r) \,. \tag{5}$$

Under a Lorentz transformation to the target system, the coordinate z transforms as $z \longrightarrow \gamma z$. Thus, strictly speaking, the S-matrix $S(b)$ is Lorentz invariant only if V transforms as the time-component of a four-vector, i.e. $V(r) \longrightarrow \gamma V(b, \gamma z)$.

The relativistic property described above is most easily seen within a folding potential model for a nucleon-nucleus collision:

$$V(\mathbf{r}) = \int dr'^3 \, \rho_T(\mathbf{r}') \, v_{NN}(\mathbf{r} - \mathbf{r}') \,, \tag{6}$$

where $\rho_T(\mathbf{r}')$ is the nuclear density of the target. In the frame of reference of the projectile, the density of the target looks contracted and particle number conservation leads to the relativistic modification of eq. 6 so that $\rho_T(\mathbf{r}') \rightarrow \gamma \rho_T(\mathbf{r}'_\perp, \gamma z')$, where $\mathbf{r}'_\perp$ is the transverse component of $\mathbf{r}'$. But the number of nucleons as seen by the target (or projectile) per unit area remains the same. In other words, a change of variables $z'' = \gamma z'$ in the integral of eq. 6 seems to restore the same eq. 6. However, this change of variables also modifies the nucleon-nucleon interaction v_{NN}. Thus, relativity introduces non-trivial effects in a potential model description of nucleus-nucleus scattering at high energies. Colloquially speaking, nucleus-nucleus scattering at high energies is not simply an incoherent sequence of nucleon-nucleon collisions. Since the nucleons are confined within a box (inside the nucleus), Lorentz contraction induces a collective effect: in the extreme limit $\gamma \rightarrow \infty$ all nucleons would interact at once with the projectile. This is often neglected in pure geometrical (Glauber model) description of nucleus-nucleus collisions at high energies, as it is assumed that the nucleons inside "firetubes" scatter independently.

Assuming that the nucleon-nucleon interaction is of very short range so that the approximation $v_{NN}(\mathbf{r} - \mathbf{r}') = J_0 \, \delta(\mathbf{r} - \mathbf{r}')$ can be used, one sees from eq. 6 that $V(\mathbf{r})$, the interaction that a nucleon in the projectile has with the target nucleus, also has similar transformation properties as the density: $V(\mathbf{r}) \rightarrow \gamma V(\mathbf{r}_\perp, \gamma z)$, i.e. $V(\mathbf{r})$ transforms as the time-component of a four-vector. In this situation, the Lorentz contraction has no effect whatsoever in the diffraction

dissociation amplitudes, described in the previous sections within the eikonal approximation. This is because a change of variables $z' = \gamma z$ in the eikonal phases leads to the same result as in the non-relativistic case, as can be easily checked from eq. 5. Of course, the delta-function approximation for the nucleon-nucleon interaction means that nucleons will scatter at once, and Lorentz contraction does not introduce any additional collective effect. This is not the case for realistic interactions with finite range and collisions at intermediate energies.

Using the eikonal approach to account for scattering of particles within the projectile, one obtains the wavefunctions for the initial and final states as

$$\Psi_i = \phi_i(\mathbf{r}) \exp(i\mathbf{k} \cdot \mathbf{R}), \qquad \Psi_f = \phi_f(\mathbf{r}) S(b) \exp(i\mathbf{k} \cdot \mathbf{R}), \tag{7}$$

where $\phi_{i,f}(\mathbf{r})$ are the initial and final probability amplitudes (wavefunctions) that a particle in the projectile is at a distance $\mathbf{r}$ from its center of mass. The particle's S-matrix, $S(b)$, accounts for the distortion due to the interaction. If we now assume that the projectile is a two-body system (e.g. a core+valence particle), we get the *diffraction dissociation* formula as follows. The wavefunction of a two-body projectile in the initial and final states is given by

$$\Psi_i = \phi_i(\mathbf{r}) \exp[i(\mathbf{k}_c \cdot \mathbf{r}_c + \mathbf{k}_v \cdot \mathbf{r}_v)], \qquad \Psi_f = \phi_f(\mathbf{r}) S_c(b_c) S_v(b_v) \exp[i(\mathbf{k}_c' \cdot \mathbf{r}_c + \mathbf{k}_v' \cdot \mathbf{r}_v)], \tag{8}$$

where now $\phi_{i,f}(\mathbf{r})$ are the initial and final intrinsic wavefunctions of the (core+valence particle) as a function of $\mathbf{r} = \mathbf{r}_1 - \mathbf{r}_2$. The relation between the intrinsic, $\mathbf{r}$, and center of mass, $\mathbf{R}$, coordinates is given in terms of the mass ratios $\beta_i = m_i/m_P$. Explicitly, $\mathbf{r}_v = \mathbf{R} + \beta_c \mathbf{r}$ and $\mathbf{r}_c = \mathbf{R} - \beta_v \mathbf{r}$. The core and valence particle S-matrices, $S_c(b_c)$ and $S_v(b_v)$, account for the distortion due to the interaction with the target.

The probability amplitude for diffraction dissociation is the overlap between the two wavefunctions above, i.e.

$$A_{(\text{diff})} = \int d^3 r_c d^3 r_v \; \phi_f^*(\mathbf{r}) \phi_i(\mathbf{r}) \, \delta(z_c + z_v) S_c(b_c) S_v(b_v) \exp[i(\mathbf{q}_c \cdot \mathbf{r}_c + \mathbf{q}_v \cdot \mathbf{r}_v)], \tag{9}$$

where $\mathbf{q}_c = \mathbf{k}_c' - \mathbf{k}_c$ is the momentum transfer to the core particle, and accordingly for the valence particle. The above formula yields the probability amplitude that the projectile starts the collision as a bound state and ends up as two separated pieces, in this case, the core and the valence particle (e.g. a proton or a neutron). All the information for the dissociation mechanism comes from the knowledge of the S-matrices, S_c and S_v. The delta-function $\delta(Z)$ was introduced in the eq. 9 to account for the fact that the S-matrices calculated in the eikonal approximation only depend on the transverse direction.

In the weak interaction limit, or perturbative limit, the phase-shifts are very small so that

$$S_c(b_c) S_v(b_v) = \exp[i(\chi_c + \chi_v)] \simeq 1 + i\chi_c + i\chi_v$$
$$= 1 - \frac{i}{\hbar v} \int V_{cT}(\mathbf{r}_c) \; dz_c - \frac{i}{\hbar v} \int V_{vT}(\mathbf{r}_v) \; dz_v. \tag{10}$$

The factor 1 does not contribute to the breakup. Thus, inserting the result above in eq. 9, we obtain

$$A_{(\text{PWBA})} \simeq \frac{1}{i\hbar v} \int d^3 r_c d^3 r_v \; \phi_f^*(\mathbf{r}) \phi_i(\mathbf{r}) [V_{cT}(\mathbf{r}_c) + V_{vT}(\mathbf{r}_v)] \exp[i(\mathbf{q}_c \cdot \mathbf{r}_c + \mathbf{q}_v \cdot \mathbf{r}_v)], \tag{11}$$

where the integrals over z_c and z_v in eq. 10 were absorbed back to the integrals over $\mathbf{r}_c$ and $\mathbf{r}_v$ after use of the delta-function $\delta(z_c + z_v)$. The above equation is nothing more than the plane-wave Born-approximation (PWBA) amplitude. However, absorption is not treated properly. For small values of $\mathbf{r}_c$ and $\mathbf{r}_v$ the phase-shifts are not small and the approximation used in eq. 10 fails. A better approximation is to assume that for small distances, where absorption is important, $S_c(b_c) S_v(b_v) \simeq S(b)$, where the right-hand side is the S-matrix for the projectile scattering as a whole on the target. Using the coordinates $\mathbf{r}$ and $\mathbf{R}$, and defining $U_{int}(\mathbf{r}, \mathbf{R}) = V_{cT}(\mathbf{r}_c) + V_{nT}(\mathbf{r}_n)$, one gets for the T-matrix

$$T_{(\text{DWBA})} = i\hbar v A_{(\text{DWBA})} \simeq \int d^3 r d^3 R \; \phi_f^*(\mathbf{r}) \exp[i\mathbf{q} \cdot \mathbf{r}] \phi_i(\mathbf{r}) U_{int}(\mathbf{r}, \mathbf{R}) S(b) \exp[i\mathbf{Q} \cdot \mathbf{R}]. \tag{12}$$

In elastic scattering, or excitation of collective modes (e.g. giant resonances), the momentum transfer to the intrinsic coordinates can be neglected and the equation above can be written as

$$T_{(\text{DWBA})} = \left\langle \chi^{(-)}(\mathbf{R}) \phi_c(\mathbf{r}) | U_{int}(\mathbf{r}, \mathbf{R}) | \chi^{(+)}(\mathbf{R}) \phi_i(\mathbf{r}) \right\rangle, \tag{13}$$

which has the known form of the DWBA T-matrix. The scattering phase space now only depends on the center of mass momentum transfer $\mathbf{Q}$. When the center of mass scattering waves are represented by eikonal wavefunctions, one has

$$\chi^{(-)*}(\mathbf{R})\,\chi^{(+)}(\mathbf{R}) \simeq S(b)\exp[i\mathbf{Q}\cdot\mathbf{R}] \ . \tag{14}$$

This shows that the PWBA and the DWBA are perturbative expansions of the diffraction dissociation formula 9.

In DWBA (or in the eikonal approximation, eq. 14), b does not have the classical meaning of an impact parameter. To obtain the semiclassical limit one goes one step further. By using eq. 12 and assuming that R depends on time so that $R = (\mathbf{b}, Z = vt)$, the semiclassical scattering amplitude is given by $A^{(i \to f)}_{(\text{semiclass})}(b) = \int d^2 b\, a^{(i \to f)}_{(\text{semiclass})}(b)\exp(i\mathbf{Q}\cdot\mathbf{b})$, where

$$a^{(i \to f)}_{(\text{semiclass})}(b) = \frac{1}{i\hbar}\,S(b)\int dt d^3 r\,\exp\left(i\omega_{if}\,t\right)\phi_f^*(\mathbf{r})\,U_{int}(\mathbf{r},t)\phi_i(\mathbf{r}) \ , \tag{15}$$

where $Q_z Z = \omega_{if}\,t$ was used.

The semiclassical probability for the transition $(i \to f)$ is obtained from the above equations after integration over $\mathbf{Q}$. One gets $P^{(i \to f)}_{(\text{semiclass})}(b) = \left|a^{(i \to f)}_{(\text{semiclass})}(b)\right|^2$, with b having now the explicit meaning of an impact parameter. Thus, $a^{(i \to f)}_{(\text{semiclass})}(b)$ is the semiclassical excitation amplitude. Equation 15 is well-known (for example in Coulomb excitation at low energies, where $U_{int} = U_C$) except that the factor $S(b)$ is usually set to one. In high energy collisions it is crucial to keep this factor, as it accounts for refraction and absorption at small impact parameters: $|S(b)|^2 = \exp\left[2\chi^{(\text{imag})}\right]$, where $\chi^{(\text{imag})}$ is calculated with the imaginary part of the optical potential. The derivation of the DWBA and semiclassical limits of eikonal methods can be easily extended to higher-orders in the perturbation V. The eikonal method includes all terms of the perturbation series in the sudden-collision limit.

The developments presented in this section show that the DWBA calculations of nuclear excitation, and the higher order terms, are implicitly included in the eikonal models. However, there is a subtle link to the optical potential, which makes the theory Lorentz covariant. Usually, the optical limit of the Glauber-eikonal series is used. In this model, no explicit reference to a nuclear potential is done; only the nucleon-nucleon cross sections and nuclear densities are used as input (see, e.g. ref. [12]). As shown above, this is also not a guarantee of Lorentz covariance. Even worse is the fact that often DWBA (and higher-order, e.g. CDCC [13, 14, 15]) calculations are used without consideration of relativistic effects. In the next section I give an example of a method (relativistic CDCC) which incorporates relativistic corrections in a continuum-discretized basis [16].

5. RELATIVISTIC CONTINUUM DISCRETIZED COUPLED-CHANNELS

Let us consider the Klein-Gordon (KG) equation with a potential V_0 which transforms as the time-like component of a four-vector [17] (here I use the notation $\hbar = c = 1$). For a system with total energy E (including the rest mass M), the KG equation can be cast into the form of a Schrödinger equation (with $\hbar = c = 1$), $\left(\nabla^2 + k^2 - U\right)\Psi = 0$, where $k^2 = \left(E^2 - M^2\right)$ and $U = V_0(2E - V_0)$. When $V_0 \ll M$, and $E \simeq M$, one gets $U = 2MV_0$, as in the non-relativistic case. The condition $V_0 \ll M$ is met in peripheral collisions between nuclei at all collision energies. Thus, one can always write $U = 2EV_0$. A further simplification is to assume that the center of mass motion of the incoming projectile and outgoing fragments is only weakly modulated by the potential V_0. To get the dynamical equations, one discretizes the wavefunction in terms of the longitudinal center-of-mass momentum k_z, using the ansatz

$$\Psi = \sum_{\alpha}\mathscr{S}_\alpha(z,\mathbf{b})\,\exp(ik_\alpha z)\,\phi_{k_\alpha}(\xi) \ . \tag{16}$$

In this equation, $(z,\mathbf{b})$ is the projectile's center-of-mass coordinate, with $\mathbf{b}$ equal to the transverse coordinate. $\phi(\xi)$ is the projectile intrinsic wavefunction and $(k,\mathbf{K})$ is the projectile's center-of mass momentum with longitudinal momentum k and transverse momentum $\mathbf{K}$. There are hidden, uncomfortable, assumptions in eq. 16. The separation between the center of mass and intrinsic coordinates is not permissible under strict relativistic treatments. For high energy collisions we can at best justify eq. 16 for the scattering of light projectiles on heavy targets. Eq. 16 is only reasonable if the projectile and target closely maintain their integrity during the collision, as in the case of very peripheral collisions.

Neglecting the internal structure means $\phi_{k_\alpha}(\xi) = 1$ and the sum in eq. 16 reduces to a single term with $\alpha = 0$, the projectile remaining in its ground-state. It is straightforward to show that inserting eq. 16 in the KG equation

$\left(\nabla^2 + k^2 - 2EV_0\right)\Psi = 0$, and neglecting $\nabla^2 \mathscr{S}_0(z, \mathbf{b})$ relative to $ik\partial_Z \mathscr{S}_0(z, \mathbf{b})$, one gets $ik\partial_Z \mathscr{S}_0(z, \mathbf{b}) = EV_0 \mathscr{S}_0(z, \mathbf{b})$, which leads to the center of mass scattering solution $\mathscr{S}_0(z, \mathbf{b}) = \exp\left[-iv^{-1}\int_{-\infty}^z dz'\, V_0(z', \mathbf{b})\right]$, with $v = k/E$. Using this result in the Lippmann-Schwinger equation, one gets the familiar result for the eikonal elastic scattering amplitude, i.e. $f_0 = -i(k/2\pi)\int d\mathbf{b}\, \exp(i\mathbf{Q}\cdot\mathbf{b})\,\{\exp[i\chi(\mathbf{b})] - 1\}$, where the eikonal phase is given by $\exp[i\chi(\mathbf{b})] = \mathscr{S}_0(\infty, \mathbf{b})$, and $\mathbf{Q} = \mathbf{K}' - \mathbf{K}$ is the transverse momentum transfer. Therefore, the elastic scattering amplitude in the eikonal approximation has the same form as that derived from the Schrödinger equation in the non-relativistic case.

For inelastic collisions we insert eq. 16 in the KG equation and use the orthogonality of the intrinsic wavefunctions $\phi_{k_\alpha}(\xi)$. This leads to a set of coupled-channels equations for $\mathscr{S}_\alpha$:

$$\left(\nabla^2 + k^2\right)\mathscr{S}_\alpha e^{ik_\alpha z} = \sum_\alpha \left\langle \alpha \left| U \right| \alpha' \right\rangle \mathscr{S}_{\alpha'}\, e^{ik_{\alpha'} z}, \tag{17}$$

with the notation $|\alpha\rangle = |\phi_{k_\alpha}\rangle$. Neglecting terms of the form $\nabla^2 \mathscr{S}_\alpha(z, \mathbf{b})$ relative to $ik\partial_Z \mathscr{S}_\alpha(z, \mathbf{b})$, eq. 17 reduces to

$$iv\frac{\partial \mathscr{S}_\alpha(z, \mathbf{b})}{\partial z} = \sum_{\alpha'} \left\langle \alpha \left| V_0 \right| \alpha' \right\rangle \mathscr{S}_{\alpha'}(z, \mathbf{b})\, e^{i(k_{\alpha'} - k_\alpha)z}. \tag{18}$$

The scattering amplitude for the transition $0 \to \alpha$ is given by

$$f_\alpha(\mathbf{Q}) = -\frac{ik}{2\pi}\int d\mathbf{b}\,\exp(i\mathbf{Q}\cdot\mathbf{b})\,\left[S_\alpha(\mathbf{b}) - \delta_{\alpha,0}\right], \tag{19}$$

with $S_\alpha(\mathbf{b}) = \mathscr{S}_\alpha(z = \infty, \mathbf{b})$. The set of equations 18 and 19 are the relativistic-CDCC equations (RCDCC).

The RCDCC equations have been used [16] to study the dissociation of ^{8}B projectiles at high energies. The energies transferred to the projectile are small, so that the wavefunctions can be treated non-relativistically in the projectile frame of reference. In this frame the wavefunctions are described in spherical coordinates, i.e. $|\alpha\rangle = |jlJM\rangle$, where j, l, J and M denote the angular momentum numbers characterizing the projectile state. Eq. 18 is Lorentz invariant if the potential V_0 transforms as the time-like component of a four-vector. The matrix element $\langle \alpha |V_0| \alpha'\rangle$ is also Lorentz invariant, and one can therefore calculate them in the projectile frame.

The longitudinal wavenumber $k_\alpha \simeq (E^2 - M^2)^{1/2}$ also defines how much energy is gone into projectile excitation, since for small energy and momentum transfers $k'_\alpha - k_\alpha = (E'_\alpha - E_\alpha)/v$. In this limit, eqs. 18 and 19 reduce to semiclassical coupled-channels equations, if one uses $z = vt$ for a projectile moving along a straight-line classical trajectory, and changing to the notation $\mathscr{S}_\alpha(z, b) = a_\alpha(t, b)$, where $a_\alpha(t, b)$ is the time-dependent excitation amplitude for a collision wit impact parameter b (see eqs. 41 and 76 of ref. [18]). The full version of eq. 19 was used in ref. [16], with relativistic corrections in both the Coulomb and nuclear potentials.

If the state $|\alpha\rangle$ is in the continuum (positive proton+^{7}Be energy) the wavefunction is discretized according to $|\alpha; E_\alpha\rangle = \int dE'_\alpha\, \Gamma(E'_\alpha)\, |\alpha; E'_\alpha\rangle$, where the functions $\Gamma(E_\alpha)$ are assumed to be strongly peaked around the energy E_α with width ΔE. For convenience the histogram set (eq. 3.6 of ref. [19]) is chosen. The inelastic cross section is obtained by solving the RCDCC equations and using $d\sigma/d\Omega dE_\alpha = |f_\alpha(\mathbf{Q})|^2\, \Gamma^2(E_\alpha)$.

Figure 2 shows the relative energy spectrum between the proton and the ^{7}Be after the breakup of ^{8}B on lead targets at 83 MeV/nucleon. The data are from ref. [20]. In this case, the calculation was restricted to $b > 30$ fm. The dotted curve is the first-order perturbation calculation, the solid curve is the RCDCC calculation, and the dashed curve is obtained with the replacement of γ by unity in the nuclear and Coulomb potentials. The difference between the solid and the dashed-curve is of the order of 4-9%.

6. CONCLUSIONS

The consequence of neglecting relativity in nuclear reactions at intermediate energies is not easy to access. The inclusion of relativity introduces non-trivial effects in semiclassical, DWBA, eikonal, and continuum discretized coupled-channels calculations. Nuclear collisions are up to now the most used probe of the internal structure of rare nuclear isotopes. To my knowledge, most experiments have been analyzed using non-relativistic theoretical methods. It might be necessary to review the results of some of these data, using a proper treatment of the relativistic corrections in the theoretical calculations used in the experimental analysis. Other improvements of the formalisms presented here
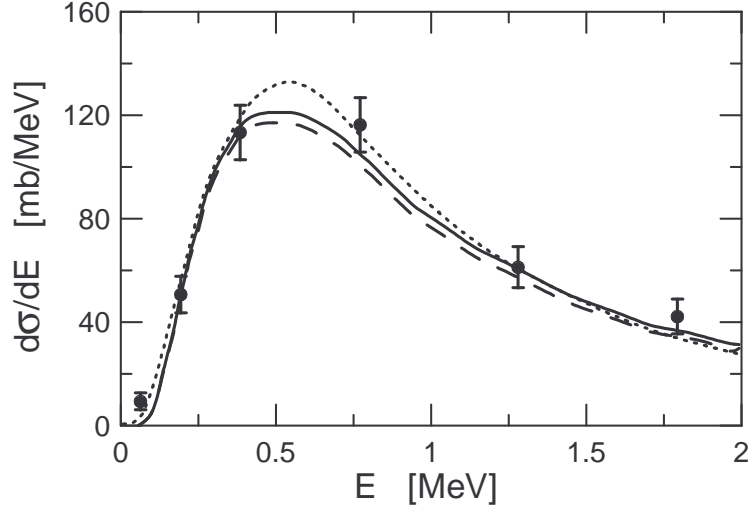
FIGURE 2. Cross sections for the dissociation reaction ^{8}B+Pb $\rightarrow$ p+^{7}Be+Pb at 83 MeV/nucleon and for $\theta_8 < 1.8^0$. Data are from ref. [20]. The dotted curve is the first-order perturbation result. The solid curve is the RCDCC calculation. The dashed curve is obtained with the replacement of γ by unity in the nuclear and Coulomb potentials.

and elsewhere needs to be assessed. The relativistic effects in the nuclear interaction has also to be studied in more depth.

Special relativity [1], one of the most precious theories of Eintein's legacy, still remains a source of intriguing effects, not always easy to tackle. Nuclear physics is full of such examples.

ACKNOWLEDGMENTS

REFERENCES

1. A. Einstein, Annalen der Physik **17** (1905) 891.
2. C.E.Aguiar, A.N.F.Aleixo and C.A.Bertulani, Phys. Rev. **C 42** (1990) 2180.
3. A.D. Fokker, Z. Phys. **58**, 386 (1929); J.A. Wheeler and R.P. Feynman, Rev. Mod. Phys. **17**, 157 (1945); **21**, 425 (1949).
4. K. Alder and A. Winther, Electromagnetic Excitation, North-Holland, Amsterdam, 1975.
5. A. Winther and K. Alder, Nucl. Phys. **A 319** (1979) 518.
6. C.A. Bertulani and G. Baur, Nucl. Phys. **A 442** (1985) 739; C.A. Bertulani and G. Baur, Phys. Rep. **163** (1988) 299.
7. A.N.F. Aleixo and C.A. Bertulani, Nucl. Phys. **A 505** (1989) 448.
8. C.A. Bertulani and A.M. Nathan, Nucl. Phys. **A 554** (1993) 158.
9. C.A. Bertulani, A. Stuchbery, T. Mertzimekis and A. Davies, Phys. Rev. **C 68**, 044609 (2003).
10. H. Scheit *et al.*, Phys. Rev. Lett. **77** (1996) 3967.
11. P. G. Hansen and J. A. Tostevin, Annu. Rev. Nucl. Part. Sci. **53**, 219 (2003).
12. C.A. Bertulani and P. Danielewicz, "Introduction to Nuclear Reactions", IOP Publishing, London, 2004, p. 419.
13. G.H. Rawitscher, Phys. Rev. **C 9**, 2210 (1974).
14. Y. Sakuragi, M. Yashiro and M. Kamimura, Prog. Theor. Phys. Suppl. **89**, 136 (1986).
15. F.M. Nunes and I.J. Thompson, Phys. Rev. **C 57**, R2818 (1998).
16. C.A. Bertulani, Phys. Rev. Lett. **94**, 072701 (2005).
17. L.G. Arnold and B.C. Clark, Phys. Lett. **B 84**, 46 (1979).
18. C.A. Bertulani, C.M. Campbell, and T. Glasmacher, Comput. Phys. Commun. **152**, 317 (2003).
19. C.A.Bertulani and L.F.Canto, Nucl. Phys. **A 540,** 328 (1992).
20. B. Davids, et al., Phys. Rev. **C 63**, 065806 (2001).